

Supplementary information for

Formation, compression and surface melting of colloidal clusters by active particles

Felix Kümmel,^a Parmida Shabestari,^a Celia Lozano,^b Giovanni Volpe^{cd} and Clemens Bechinger^{ab}

1 Sample preparation

A quadratic particle confinement with an area of $0.5 \times 0.5 \text{ cm}^2$ and a height of about $6 \mu\text{m}$ is produced on a glass substrate. This is achieved by depositing a thin layer of the photoresist SU-8 2005 on the substrate by a spin coating process at 2000 rpm. Afterwards the square structures are created by a photolithographic process (soft lithography). Then, the colloidal suspension is injected into the cavity, enclosed by a cover glass and finally sealed with epoxy glue. Variations of the particle density in the sample cell is achieved by changing the particle concentration of the injected suspension. In order to reduce particle sticking to surfaces, the glass substrates is rendered negatively charged by an oxygen plasma treatment prior to cell assembly.

2 Particle tracking

In Fig. S1, a pre-analysis microscope image of a mixture of active and passive colloids is shown. Here, active Janus particles appear darker than passive colloids due to their absorptive carbon coating. Because the cap covers only half of a particle, the optical contrast of active particles in the video images depends on their orientation and thus slightly changes over time due to rotational diffusion. To reliably distinguish active from passive particles under such conditions, we first determine the positions of all particles (by tracking their characteristic dark spherical edges) and determine the brightness inside each tracked ring. In a second step we calculate the mean brightness for each particle trajectory. When this mean brightness is below a certain threshold value (which depends on the details of the imaging conditions), the trajectory is associated to an active particle. This approach works reliably for all particle concentrations used in our experiments.

3 Dynamics of cluster formation

The compression and merging of clusters at $0.48 \pm 0.08 < \eta_p \leq 0.62 \pm 0.05$ can be quantified by measuring the mean particle distance within activity-induced clusters over time. In Fig. S2, we compare the decrease of the mean inter-particle distance inside activity-induced clusters for $Pe = 8.8 \pm 2.7$, 20.3 ± 2.7 and 29.8 ± 2.7 . The temporal change is well described by an exponential decay (solid lines), whose saturation value and decay time strongly decrease with increasing Peclet number.

In Fig. S3 we show the fraction F_C of particles inside clusters for $\eta_p = 0.4$ and $\eta_p = 0.6$.

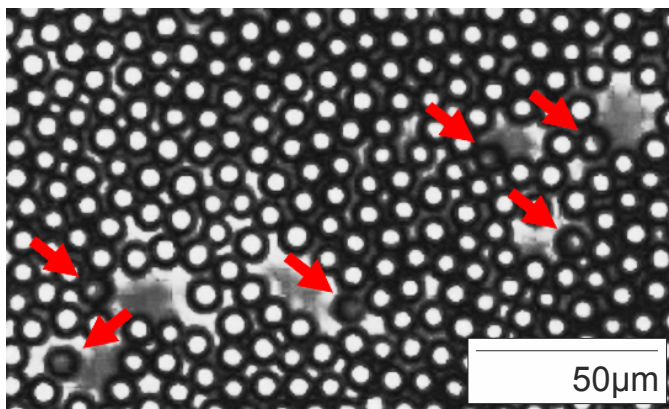


Figure S 1 Microscope image showing a mixture of active and passive particles at $\eta_p = 0.62$. Due to their carbon caps, active particles, which are indicated by arrows, appear darker and can therefore be optically distinguished from passive particles.

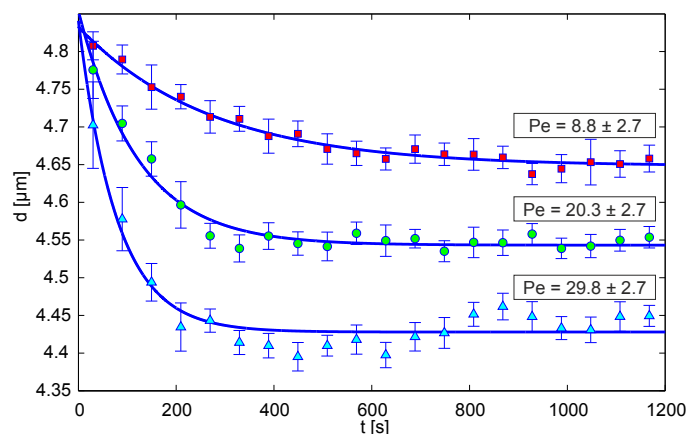


Figure S 2 Experimentally measured average mean inter-particle distance within activity-induced clusters over time for $\eta_p \approx 0.61$ (c.f. Figs. 2(e) and 2(f)) obtained (from top to bottom) for $Pe = 8.8 \pm 2.7$, 20.3 ± 2.7 and 29.8 ± 2.7 . Each point represents the mean value averaged over 60 s. The solid lines correspond to shifted exponential fits with time constants $\tau = (270 \pm 24)$ s, (122 ± 14) s and (78 ± 12) s.

4 Comparison with numerical simulations

The results obtained by computer simulations for the temporal change of the passive particle distribution are shown in Fig. S4. The color code is identical to that of Fig. 2. Similarly to the experimental results shown in Fig. 2, we observe different structural changes in the passive particle distribution induced by the presence of the active particles depending on η_p . In short, at $\eta_p = 0.25$, there is no visible change in the passive particle dis-

^a 2. Physikalisches Institut, Universität Stuttgart, D-70569 Stuttgart, Germany.

^b Max-Planck-Institut für Intelligente Systeme, D-70569 Stuttgart, Germany.

^c Soft Matter Lab, Department of Physics, Bilkent University, Ankara 06800, Turkey.

^d UNAM - National Nanotechnology Research Center, Bilkent University, Ankara 06800, Turkey.

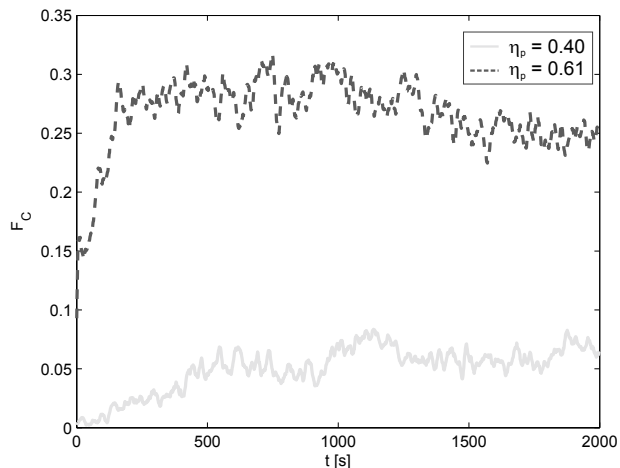


Figure S 3 Experimentally measured fraction F_C of particles inside clusters over time for different values of η_p at $Pe = 20$.

tribution (Figs. S3(a) and S3(b)). For $\eta_p = 0.50$, we observe the activity-induced formation of small clusters (Figs. S3(c) and 3(d)). The compression and merging of existing clusters is visible at $\eta_p = 0.61$ (Figs. S3(e) and S3(f)). At $\eta_p = 0.89$ (Figs. S3(g) and S3(h)), it is possible to observe the surface melting of existing crystals by active particles, leading to a rearrangement of the crystalline domains. Furthermore, the preferential motion of active particles from inside crystalline areas to the grain boundaries of the domains is clearly visible by comparing their initial and final positions.

In Fig. S5(a) we have analyzed the evolution of the number of the clusters N_C , finding results in agreement with the experimental data shown in Fig. 3. In particular, we find an increase of the number of clusters for relatively small η_p , which is consistent with activity-induced cluster formation. At higher η_p , the number of clusters decreases due to cluster merging. In both cases, the simulations reach a steady state as seen by the convergence of the probability distributions and the complementary cumulative distribution function in Figs. S4(b) and S4(c).

5 Growth of crystalline domains

For very large simulation times and high particle densities, we observe the formation of large, defect-free colloidal domains. This is due to the accumulation of active particles along grain boundaries which lead to the permanent melting and recrystallization of such regions. This eventually leads to the macroscopic shift of grain boundaries and the growth of crystalline regions at expense of adjacent ones as shown in Fig. S6.

6 Supporting video information

SV1 - Active particles moving along a grain boundary inside a dense colloidal suspension with $\eta_p = 0.80$ and $Pe \approx 20$. The video has been accelerated by $180\times$ (original length: 1800 s). Trajectories of active particles have been superimposed as blue lines.

SV2 - Active particle moving inside a crystalline domain of a dense colloidal suspension with $\eta_p = 0.80$ and $Pe \approx 20$. The video

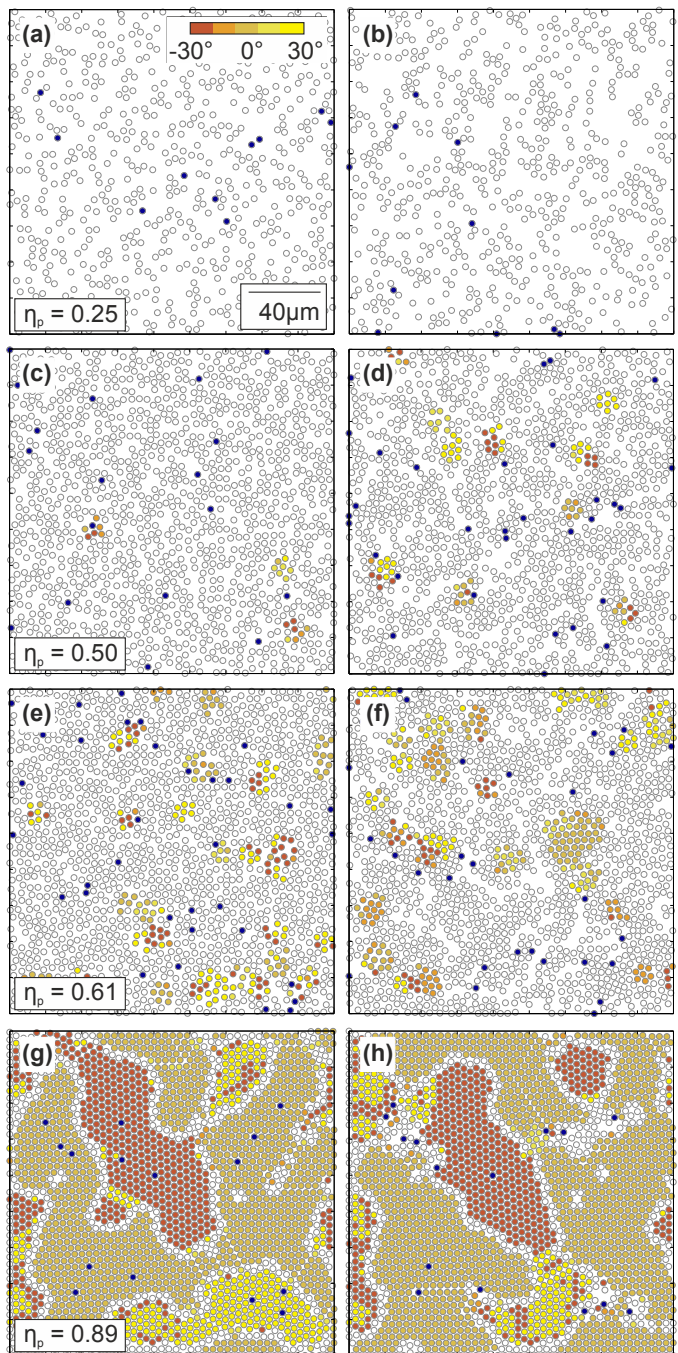


Figure S 4 Numerical simulations corresponding to Fig. 2. Temporal change of the passive particle distribution for different values of η_p at $Pe = 20$ obtained by computer simulations. The color code corresponds to the bond orientation of particles inside clusters (as defined in the main text) relative to the horizontal axis. Particles not belonging to clusters are marked as open circles. Active particles are shown as blue bullets. (a), (b) $\eta_p = 0.25$; (c), (d) $\eta_p = 0.5$; (e), (f) $\eta_p = 0.61$; (g), (h) $\eta_p = 0.89$. (a), (c), (e), (g) $t = 0$; (b), (d), (f), (h) 2000 s.

has been accelerated by $180\times$ (original length: 1800 s). The trajectory of the active particle has been superimposed as a blue line.

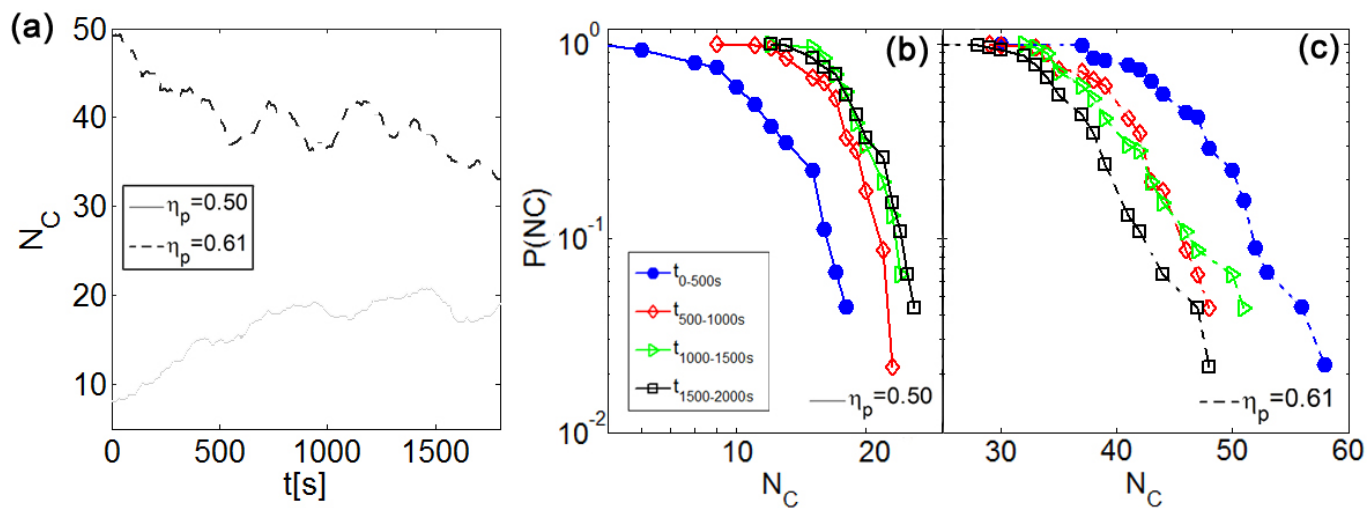


Figure S 5 (a) Number of cluster N_C for different values of η_p . (b)-(c) CCDFs of N_C for various time series as indicated in the legend for (b) $\eta_p = 0.50$ and (c) $\eta_p = 0.61$. The Peclet number is $Pe = 20$.

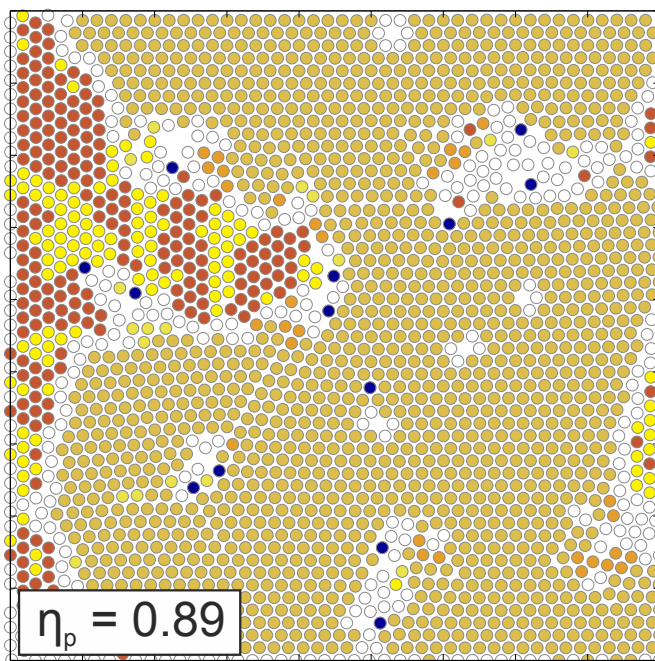


Figure S 6 Snapshot of the configuration corresponding to Figs. S4 (g) and (h) after a simulation time of 8000 s. The color code corresponds to the bond orientation of particles inside clusters (as defined in the main text) relative to the horizontal axis. Particles not belonging to clusters are marked as open circles. Active particles are shown as blue bullets.